THE JOURNAL OF PHYSICAL CHEMISTRY LETTERS
A JOURNAL OF THE AMERICAN CHEMICAL SOCIETY

pubs.acs.org/JPCL

Letter

Interfacial Barrier of Ion Transport in Poly(ethylene oxide)–$Li_7La_3Zr_2O_{12}$ Composite Electrolytes Illustrated by ^{6}Li-Tracer Nuclear Magnetic Resonance Spectroscopy

Jia He, Huixin Chen, Dawei Wang, Qian Zhang,* Guiming Zhong,* and Zhangquan Peng*

Cite This: *J. Phys. Chem. Lett.* 2022, 13, 1500–1505

Read Online

ACCESS | Metrics & More | Article Recommendations | Supporting Information

ABSTRACT: Fundamental understanding of the lithium-ion transport mechanism in polymer–inorganic composite electrolyte is crucially important for the rational design of composite electrolytes for solid-state batteries. In this work, the Li^+ ion transport pathway in a model composite electrolyte of PEO containing sparsely dispersed LLZO (PEO–LLZO) was studied by an advanced characterization technique, i.e., ^{6}Li-tracer NMR spectroscopy. By analyzing the ^{6}Li distribution within the PEO–LLZO composite at the end of the discharge of an electrochemical cell of ^{6}Li | PEO–LLZO | stainless steel with a fixed capacity (less than the total amount of the Li^+ in the composite) at various current densities, it is found that the interfacial barrier between LLZO and PEO could cause a reduced Li^+ flux through LLZO, particularly at high current densities, and therefore plays a critical role in determining the Li^+ transport pathway in the composite electrolyte. This work provides an intuitive picture of Li^+ ion transport in a polymer–inorganic composite electrolyte that is helpful to optimize and design better composite electrolytes.

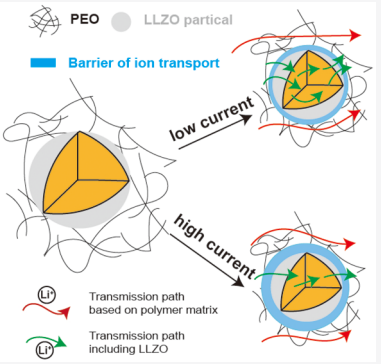

Developing rechargeable lithium batteries with higher energy density and greater safety has been a critical field in electrochemical storage systems. Solid-state electrolytes (SSEs) with nonflammable characteristics in contrast to traditional liquid electrolytes with serious risks for leakage and flammability of organic solvents have become the research emphasis.[1−3] SSEs can greatly improve the safety and match the lithium metal anode, thus enhancing the energy densities of corresponding solid-state lithium batteries.[4,5]

Among various SSEs, polymer electrolytes (such as poly(ethylene oxide) (PEO),[6] polyvinylidene fluoride (PVDF),[7] poly(methyl methacrylate) (PMMA),[8] and polyacrylonitrile (PAN)[9] based electrolytes) with flexibility and thus good contact with electrodes and easily scalable production have presented promising industrial application prospects and compatibility with commercial lithium-ion batteries. However, lithium ions mainly transmit through the segmental movement of the amorphous domain in polymer electrolytes, resulting in a poor room-temperature ionic conductivity, which has been a decisive issue hindering their further application. Many efforts have been made to reduce the glass transition temperatures (T_g) of polymer electrolytes by adding plasticizers, including inorganic inert (Al_2O_3, SiO_2, TiO_2, etc.),[10−12] inorganic electrolytes ($Li_7La_3Zr_2O_{12}$, $Li_{0.34}La_{0.56}TiO_3$, $Li_{10}GeP_2S_{12}$, $Li_{1.4}Al_{0.4}Ti_{1.6}(PO_4)_3$, etc.),[13−16] etc., to enhance the segmental motion. The interaction between the surface of doped particles and polymer components has been reported to be a key factor influencing the dissociation degree of Li^+ ions.[17,18] It may increase the proportion of transferable lithium ions in the composite electrolyte, thus raising the ionic conductivity. The morphology of the inorganic filler is another important factor. Filling of nanowires always exhibits a greater improvement in comparison to nanoparticles.[19] Moreover, the addition of orientated distributed nanowires has been verified for a higher ionic conductivity than that of disordered nanowires,[20] which probably originates from the shortened Li^+ transmission distance in the electrolyte owing to the directional transport of Li^+ along the alignment.[21]

Many strategies have been developed; however, it is essential to carefully investigate the elementary ion-transfer processes and deeply understand the ion transport pathways and the corresponding barriers in the electrolytes, especially as inorganic ionic conductive fillers are employed. The Li^+-conducting inorganic particles and the inorganic/polymer interfaces possibly participate in the ion-transfer process, leading to more complex lithium-ion transport pathways. Several techniques have been applied to study the properties and the transport mechanisms in polymer and composite polymer electrolytes. Bruce et al. successfully obtained the spiral cylindrical structure of crystalline PEO polymer electrolyte by applying XRD,[22] which revealed that lithium-

Received: December 15, 2021
Accepted: January 28, 2022
Published: February 7, 2022

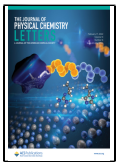

https://doi.org/10.1021/acs.jpclett.1c04085
J. Phys. Chem. Lett. 2022, 13, 1500–1505

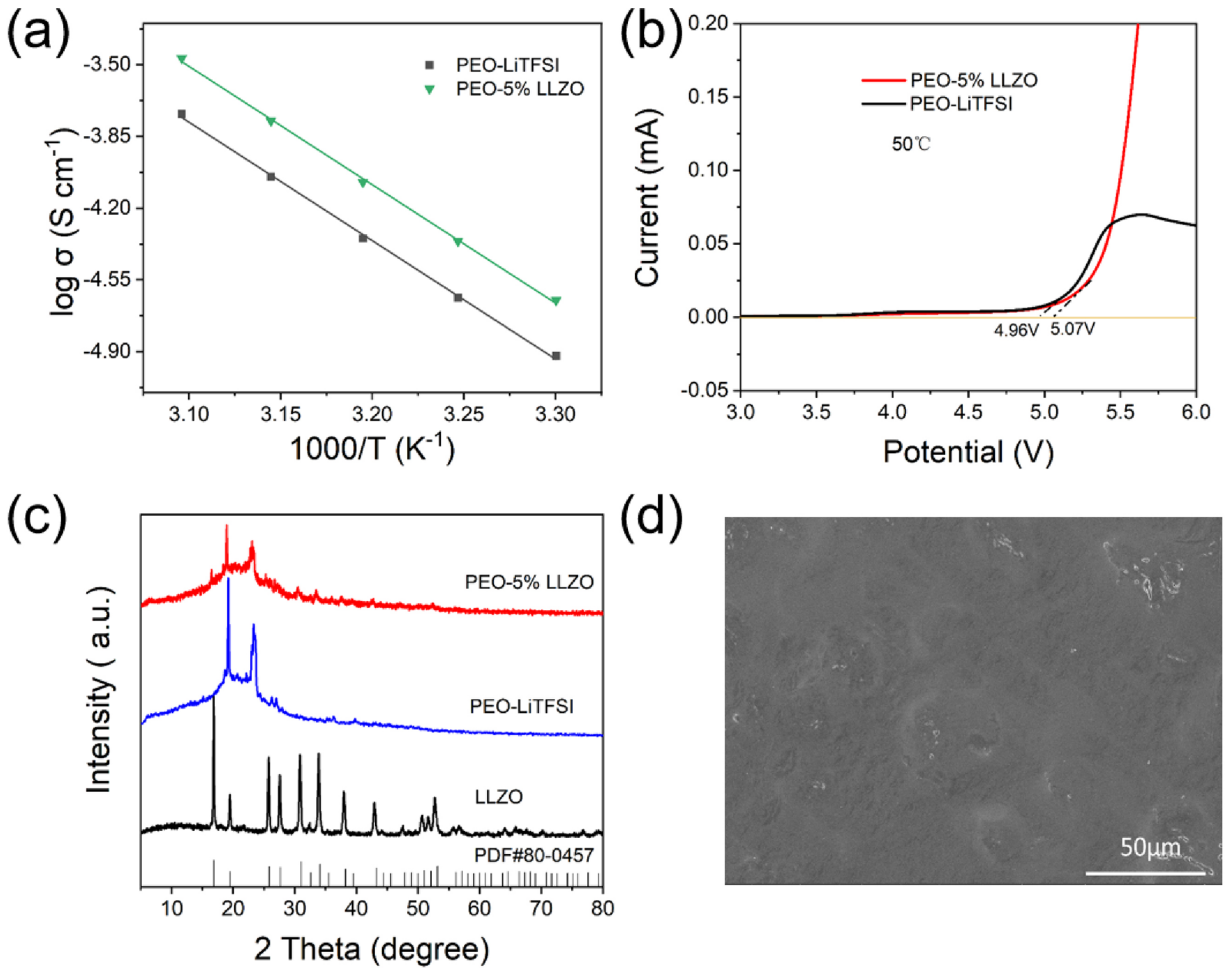

Figure 1. (a) Arrhenius plots, (b) LSV (linear sweep voltammetry) curves, and (c) XRD patterns of LLZO, PEO-LiTSFI, and PEO-5%LLZO composite electrolytes. (d) SEM image of PEO-5%LLZO electrolyte.

ion resides in the cylindrical structure but does not coordinate with anions. Saboungi et al. observed that Li^+ involves two or three different motions in the nanosecond time-scale in polymer electrolytes by using quasi-elastic neutron scattering.[23] Theoretical calculations also have been employed to analyze the relationship between ionic conductivity of multiphase composite electrolyte and filler content. Effective medium theory (EMT)[15] and percolation theory[16] can predict the atomic-level ion conduction of materials. However, the conduction mechanism from the physical and chemical levels is difficult to determine.[24]

Recently, ^{6}Li-tracer NMR spectroscopy was applied and presents great superiority to track the Li^+ transport pathways. Through cycling the ^{6}Li | SSEs | ^{6}Li symmetric cell along with the ^{6}Li NMR spectroscopy, Zheng et al. successfully tracked the Li^+ transmission path in PEO-50 wt %LLZO (LLZO means $Li_7La_3Zr_2O_{12}$)[25] and found that the lithium ion tends to pass through the LLZO ceramic phase rather than the PEO−LLZO interface or PEO phase in such an electrolyte. However, Yang et al. and Zheng et al. revealed the critical contribution of the interfacial transport in PVDF-$Li_{1.4}Al_{0.4}Ti_{1.6}(PO_4)_3$ nanowires[5] and PAN-5%LLZO nanowires[26] by utilizing a similar approach. Understanding of the decisive factor for the preferential ion transport pathway is still insufficient and thus crucially necessary for a rational design of the composite polymer electrolytes. Investigation of each elementary ion transport process and the corresponding transfer barrier in the composite electrolytes may possibly provide effective hints. We propose that quantitative analysis with the determined amount of ^{6}Li exchange is very important to deeply realize the Li^+ transport as ^{6}Li-tracer NMR spectroscopy is applied. ^{7}Li from the electrolyte probably deposits and reenters into the electrolyte, and the inactive components may be produced in the electrolyte or on the surface of ^{6}Li during cycling of the ^{6}Li | SSEs | ^{6}Li cell, causing deviation, especially for the comparison samples.

In this work, we employ a modification of the ^{6}Li-tracer NMR method for solid-state electrolytes. Through single equivalent ^{6}Li isotope exchange at different current densities, the transport mechanism of lithium ion in the composite electrolyte was analyzed qualitatively and quantitatively. This method can help to distinguish the rapid transport pathways and the barrier influencing the transport properties.

We applied PEO-5%LLZO electrolyte as the model, which shows the highest ionic conductivity among the prepared PEO-x%LLZO (x = 2, 5, 10, 15%) composite electrolytes (Figures 1a and S1a). The linear sweep voltammetry shows PEO-5% LLZO electrolyte has a larger electrochemical stability window (Figure 1b), confirming the positive effect of the LLZO filler, which is consistent with previous results.[27] The successful addition of LLZO in the electrolyte is further verified by XRD patterns (Figure 1c), which clearly evidence the reduced

https://doi.org/10.1021/acs.jpclett.1c04085
J. Phys. Chem. Lett. 2022, 13, 1500−1505

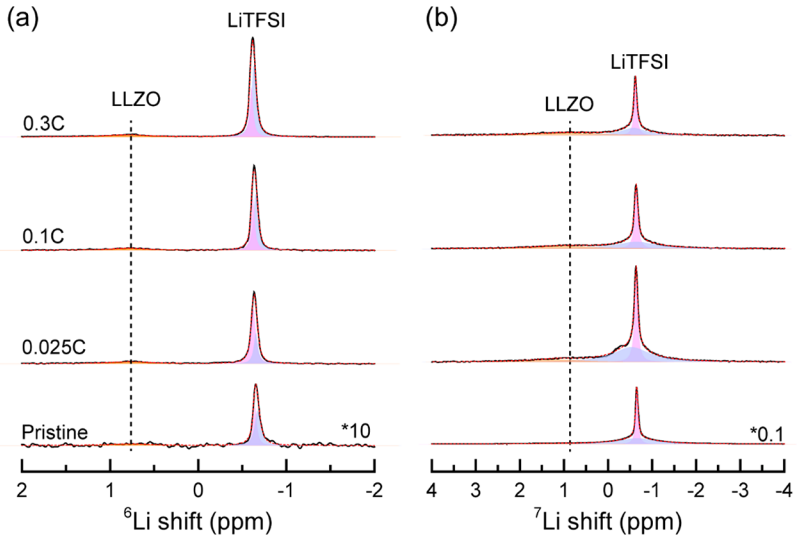

Figure 2. (a) ^{6}Li and (b) ^{7}Li NMR spectra of the PEO-5%LLZO electrolytes after ^{6}Li → ^{7}Li tracer-exchange experiment at 50 °C.

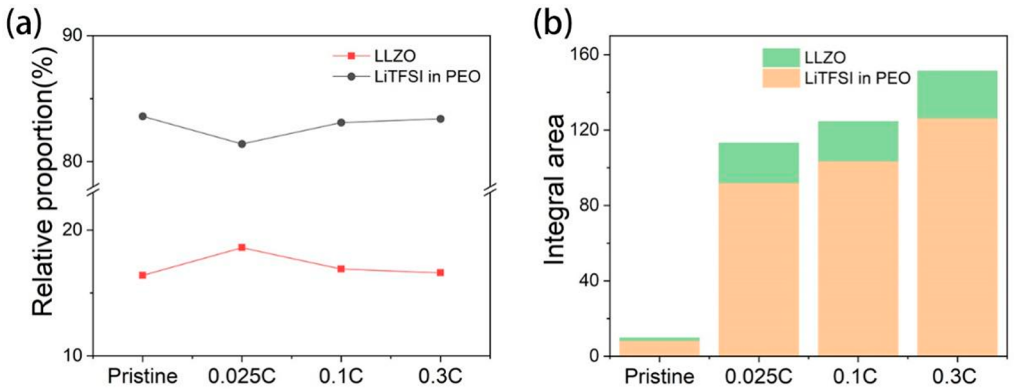

Figure 3. (a) The relative proportion and (b) the absolute content changes of ^{6}Li signals for components in ^{6}Li-exchange PEO-5%LLZO electrolytes calculated from the ^{6}Li NMR spectra.

crystallinity of the electrolyte with the addition of LLZO. In addition, SEM and EDS mapping images of the composite electrolyte display a smooth surface and an even distribution of La and Zr elements in the LLZO material (Figures 1d and S1b–d). Previous work has demonstrated that less filler (<20 wt %) may not form a percolation network.[28]

For ^{6}Li-tracer NMR, we first assembled the ^{6}Li | Polymer | SS (stainless steel) cells, which were discharged at three current densities of 0.025*C*, 0.1*C*, 0.3*C* (1*C* indicates the current density applied as the capacity equals to the charge of total lithium ions in the electrolyte in 1 h) with a determining capacity at 50 °C. The capacity was set to be a quarter of the charge of Li^{+} content in the electrolyte, expecting to ensure a constant ^{6}Li-substition proportion in the polymer electrolytes. All the spectra are normalized by acquisition number scans and sample mass for a rational comparison. Figure 2a depicts the ^{6}Li NMR spectra and corresponding fitting plots of as-prepared and ^{6}Li-exchanged PEO-5%LLZO electrolytes. The resonance at −0.78 ppm is attributed to LLZO, and the signal at approximately −0.63 ppm is due to the LiTFSI in PEO, which can be deconvoluted into two peaks assigned to the LiTFSI in crystalline and amorphous PEO phases, respectively. The spectra obviously exhibit that these ^{6}Li signals are greatly enhanced for the ^{6}Li-exchanged electrolytes compared to the pristine sample. And the ^{7}Li NMR spectra display a contrasting trend, identifying the exchange of ^{6}Li in the electrolytes.

Both the ^{6}Li and ^{7}Li NMR spectra are carefully fitted by using three peaks. It shows that the areal ratios of LLZO, LiTFSI in amorphous, and crystalline PEO phases in the pristine electrolyte are 16.4%, 49.1%, and 34.5%, respectively (Table S1). The calculated proportion of LLZO according to the fitting result of ^{6}Li NMR is lower than that from the feed value in the synthesis process. This is probably due to the loss of LLZO during preparation and the much shorter spin–spin relaxation time of LLZO in comparison to that of LiTFSI in the PEO phase. Accordingly, the composite polymer electrolyte films prepared at the same time and an identical acquisition parameter were applied to exclude the possible errors, thus obtaining comparable quantitative NMR spectra among samples. It is worth noting that the composite electrolytes were ^{6}Li-exchanged at 50 °C and the spectra were ex situ acquired at room temperature; thus, the proportions of LiTFSI signals in amorphous and crystalline PEO phases have been probably changed. Besides, the overlapping of the ^{7}Li signals may also cause large errors. Therefore, two signals from LLZO and LiTFSI in the ^{6}Li NMR spectra are mainly employed for discussion. Figure 3 and Table S1 exhibit the analysis results of ^{6}Li NMR spectra. It shows that the ^{6}Li content of LLZO in ^{6}Li NMR spectra is enhanced

https://doi.org/10.1021/acs.jpclett.1c04085
J. Phys. Chem. Lett. 2022, 13, 1500−1505

from 16.4% to 18.6% as ^{6}Li-substitution current density of 0.025C is applied, while the values (16.9% and 16.6%) are almost the same as that with the pristine when utilizing higher current densities of 0.1C and 0.3C. The tendency is further verified by another batch of samples (Figure S2 and Table S3), demonstrating the results of ^{6}Li content of 18.3% and 15.9% for LLZO in the ^{6}Li-exchanged electrolytes with current densities of 0.05C and 0.3C, respectively. It is worth mentioning that the ^{6,7}Li signals of LiTFSI in Figures 2 and S2 shift slightly, which is due to the various Li^+ solvation effects caused by the distinct residual solvent in different batches of samples. This result indicates that although the transport channel involved with LLZO is still unobstructed, the enhanced ion transport effect in the LLZO phase has been weakened at high current. It is known that LLZO presents much higher ionic conductivity than PEO electrolytes and thus a lower ion-transfer barrier. However, it reveals that the transport channel in LLZO has priority only at a very low current density. The change of ion-transfer barrier under higher current densities should be considered. The space charge layer (SCL) on the interface between PEO and LLZO, and the corresponding ion transport barrier could be enhanced as higher current densities are utilized,[29,30] thus confining the transfer of Li^+ from polymer phase to inorganic phase. Hence, the space charge layer between the LLZO and PEO phase and the relevant interfacial transport are probably the key factors causing reduced ^{6}Li substitution in the LLZO component.

Beyond the above changes of the relative proportions of components in the composite, we unexpectedly find that the absolute intensities of ^{6}Li signals in the ^{6}Li-substituted samples at different current densities change even with the identical capacity, as evidenced in Figure 3b and Tables S2−S4. The total integral area of ^{6}Li signals is enhanced by 11 times for the PEO-5%LLZO-0.025C sample in comparison to that for the pristine electrolyte, while the signal enhancement for PEO-5% LLZO-0.1C and 0.3C samples are 12.8 and 15.6, respectively. The results indicate that the ^{6}Li-exchanged amount in polymer electrolytes by using the ^{6}Li | SSEs | SS cell will be increased at a higher current density even with an identical normalized capacity (less than the total amount of the Li^+ in the composite). There are probably several factors for the enhanced intensities of ^{6}Li signals in the samples ^{6}Li-substituted at higher current density. First, it is known that the microscopic expression of the current is

$$I = neSv$$

where n represents the number of free charges per unit volume, e is the amount of electricity of the free charge, S indicates the cross-sectional area of the conductor, and v is the rate at which the free charge moves perpendicular to the electrolyte plane. Thus, the current means the amount of charge per unit time passing through the interface. We have to note that the actual polymer membrane is not an ideal plane and has a certain thickness. Therefore, the content of ^{6}Li in the electrolyte is the integral of the $^6Li^+$ passing through the cross-sectional area per unit time and the thickness of the film. The larger the current, the greater the ion flux on the cross section. Besides, the concentration gradient caused by the enhancement of the space charge layer between the electrode and the polymer electrolyte possibly aggravates the deviation of the signal intensity.

These results reveal the significance of the interfacial transport process in polymer electrolytes, in particular as the extra electric field is applied. To the best of our knowledge, the transmission pathway of Li^+ through the composite polymer is composed of the following elementary processes: Li^+ transport across the PEO phase (LiTFSI), bulk LLZO, the interface between LLZO and PEO, and the interface between membrane and electrodes.[25,26,31] The ion transport pathways in composite electrolytes could be varied as these transport barriers are changed (Figure 4). We have known that LLZO

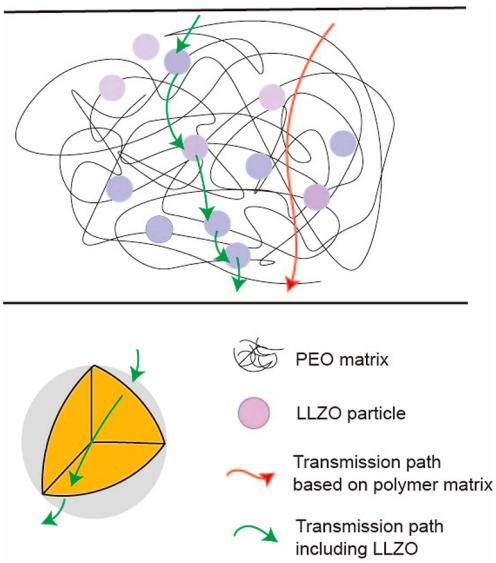

Figure 4. Schematics of the Li-ion transport pathways in the PEO−LLZO composite electrolytes.

has higher ionic conductivity than PEO and thus is an important component for the ion transport properties of the composite electrolytes. Nonetheless, the processes involving the ion transport through the interface between PEO and LLZO and the PEO phase possibly become the critical step for PEO-5%LLZO. The enhanced ion transport barrier due to the SCL possibly changes the ion transport pathways. In addition, the most sluggish ion-transfer process could be the decisive factor as ions transmit through the electrolytes by several elementary steps in series. In contrast, the fastest ion-transfer process is probably the most critical point that determines the ion transmission property as these elementary transfer processes are parallel. The practical ion transport mechanisms may be more complex, depending on the competition of elementary transport steps. This may explain the reported various preferential ion transport pathways for different composite electrolytes.[5,25,26] A relatively high interfacial transfer barrier between the polymer phase and the plasticizer, combined with the continuous filler (e.g., nanowires), possibly creates a preferential interfacial transport pathway. Therefore, the compatibility between components in the composite electrolytes and the SCL should be seriously addressed to offer a high-performance electrolyte for an excellent high-rate performance.

In summary, we present a modification of the ^{6}Li-tracer NMR method to quantify the ion transport pathways in composite electrolytes and distinguish the critical step influencing the ion transport properties. Our results demonstrate that the interfacial ion transport barrier (such as space charge layer) in the composite electrolyte should be seriously addressed, which could cause the change of ion transport

https://doi.org/10.1021/acs.jpclett.1c04085
J. Phys. Chem. Lett. 2022, 13, 1500−1505

mechanisms at different current densities. In addition, we discussed elementary ion-transfer processes in the composite electrolytes, illustrating that the varying barriers of the elementary transport processes generate different preferential ion transport pathways.

■ ASSOCIATED CONTENT

Supporting Information

The Supporting Information is available free of charge at https://pubs.acs.org/doi/10.1021/acs.jpclett.1c04085.

Experimental method, Arrhenius plots, SEM and EDS images, ^{6,7}Li NMR spectra for another batch of samples, and additional tables as described in the text (PDF)

■ AUTHOR INFORMATION

Corresponding Authors

Qian Zhang − *Key Laboratory of Power Batteries and Relative Materials, Jiangxi University of Science and Technology, Ganzhou 341000 Jiangxi, China*; Email: zhangqian@jxust.edu.cn

Guiming Zhong − *Laboratory of Advanced Spectroelectrochemistry and Li-ion Batteries, Dalian Institute of Chemical Physics Chinese Academy of Sciences, Dalian 116023 Liaoning, China; CAS Key Laboratory of Design and Assembly of Functional Nanostructures, Fujian Provincial Key Laboratory of Nanomaterials, Fujian Institute of Research on the Structure of Matter, Chinese Academy of Sciences, Fuzhou 350002 Fujian, China; Xiamen Key Laboratory of Rare Earth Photoelectric Functional Materials, Xiamen Institute of Rare Earth Materials, Haixi Institutes, Chinese Academy of Sciences, Xiamen 361021 Fujian, China;* orcid.org/0000-0003-2313-4741; Email: gmzhong@dicp.ac.cn

Zhangquan Peng − *Laboratory of Advanced Spectroelectrochemistry and Li-ion Batteries, Dalian Institute of Chemical Physics Chinese Academy of Sciences, Dalian 116023 Liaoning, China; Tianmu Lake Institute of Advanced Energy Storage Technologies Co. Ltd., Liyang 213300 Jiangsu, China;* orcid.org/0000-0002-4338-314X; Email: zqpeng@dicp.ac.cn

Authors

Jia He − *Key Laboratory of Power Batteries and Relative Materials, Jiangxi University of Science and Technology, Ganzhou 341000 Jiangxi, China; CAS Key Laboratory of Design and Assembly of Functional Nanostructures, Fujian Provincial Key Laboratory of Nanomaterials, Fujian Institute of Research on the Structure of Matter, Chinese Academy of Sciences, Fuzhou 350002 Fujian, China; Xiamen Key Laboratory of Rare Earth Photoelectric Functional Materials, Xiamen Institute of Rare Earth Materials, Haixi Institutes, Chinese Academy of Sciences, Xiamen 361021 Fujian, China*

Huixin Chen − *CAS Key Laboratory of Design and Assembly of Functional Nanostructures, Fujian Provincial Key Laboratory of Nanomaterials, Fujian Institute of Research on the Structure of Matter, Chinese Academy of Sciences, Fuzhou 350002 Fujian, China; Xiamen Key Laboratory of Rare Earth Photoelectric Functional Materials, Xiamen Institute of Rare Earth Materials, Haixi Institutes, Chinese Academy of Sciences, Xiamen 361021 Fujian, China*

Dawei Wang − *Key Laboratory of Automobile Materials of Ministry of Education & School of Materials Science and Engineering, Jilin University, Changchun 130025 Jilin, China*

Complete contact information is available at: https://pubs.acs.org/10.1021/acs.jpclett.1c04085

Notes

The authors declare no competing financial interest.

■ ACKNOWLEDGMENTS

This work was financially supported by National Nature Science Foundation of China (Grant Nos. 21905314, 21825202, 21733012, 92045302, and 21603231); Newton Advanced Fellowships (NAF/R2/180603); "Scientist Studio Funding" from Tianmu Lake Institute of Advanced Energy Storage Technologies Co., Ltd; and the Science and Technology Service Network Initiative from Chinese Academy of Science (STS 2020T3022). G.Z. acknowledges the support from the National Science Foundation Cooperative Agreement No. DMR-1644779 and the State of Florida. D.W. acknowledges support from the Fundamental Research Funds for the Central Universities, JLU.

■ REFERENCES

(1) Miller, T. F., III; Wang, Z.-G.; Coates, G. W.; Balsara, N. P. Designing Polymer Electrolytes for Safe and High Capacity Rechargeable Lithium Batteries. *Acc. Chem. Res.* **2017**, *50*, 590−593.

(2) Jiang, T. L.; He, P. G.; Wang, G. X.; Shen, Y.; Nan, C. W.; Fan, L. Z. Solvent-Free Synthesis of Thin, Flexible, Nonflammable Garnet-Based Composite Solid Electrolyte for All-Solid-State Lithium Batteries. *Adv. Energy. Mater.* **2020**, *10*, 1903376.

(3) Lee, S. Y.; Shangguan, J. Y.; Alvarado, J.; Betzler, S.; Harris, S. J.; Doeff, M. M.; Zheng, H. M. Unveiling the Mechanisms of Lithium Dendrite Suppression by Cationic Polymer Film Induced Solid-Electrolyte Interphase Modification. *Energy Environ. Sci.* **2020**, *13*, 1832−1842.

(4) Xu, H. T.; Zhang, H. R.; Ma, J.; Xu, G. J.; Dong, T. T.; Chen, J. C.; Cui, G. L. Overcoming the Challenges of 5 V Spinel $LiNi_{0.5}Mn_{1.5}O_4$ Cathodes with Solid Polymer Electrolytes. *ACS Energy Lett.* **2019**, *4*, 2871−2886.

(5) Yang, K.; Chen, L.; Ma, J.; Lai, C.; Huang, Y.; Mi, J.; Biao, J.; Zhang, D.; Shi, P.; Xia, H.; Zhong, G.; Kang, F.; He, Y. B. Stable Interface Chemistry and Multiple Ion Transport of Composite Electrolyte Contribute to Ultra-long Cycling Solid-State $Li-Ni_{0.8}Co_{0.1}Mn_{0.1}O_2$/Lithium Metal Batteries. *Angew. Chem. Int. Ed.* **2021**, *60*, 24668−24675.

(6) Zhang, J. X.; Zhao, N.; Zhang, M.; Li, Y. Q.; Chu, P. K.; Guo, X. X.; Di, Z. F.; Wang, X.; Li, H. Flexible and Ion-Conducting Membrane Electrolytes for Solid-State Lithium Batteries: Dispersion of Garnet Nanoparticles in Insulating Polyethylene Oxide. *Nano Energy* **2016**, *28*, 447−454.

(7) Xue, C.; Zhang, X.; Wang, S.; Li, L.; Nan, C. W. Organic-Organic Composite Electrolyte Enables Ultralong Cycle Life in Solid-State Lithium Metal Batteries. *ACS Appl. Mater. Interfaces* **2020**, *12*, 24837−24844.

(8) Liang, B.; Tang, S. Q.; Jiang, Q. B.; Chen, C. S.; Chen, X.; Li, S. L.; Yan, X. H. Preparation and Characterization of PEO-PMMA Polymer Composite Electrolytes Doped with Nano-Al_2O_3. *Electrochim. Acta* **2015**, *169*, 334−341.

(9) Hu, C.; Shen, Y.; Shen, M.; Liu, X.; Chen, H.; Liu, C.; Kang, T.; Jin, F.; Li, L.; Li, J.; Li, Y.; Zhao, N.; Guo, X.; Lu, W.; Hu, B.; Chen, L. Superionic Conductors via Bulk Interfacial Conduction. *J. Am. Chem. Soc.* **2020**, *142*, 18035−18041.

(10) Krawiec, W.; Scanlon, L.G.; Fellner, J.P.; Vaia, R.A.; Vasudevan, S.; Giannelis, E.P. Polymer Nanocomposites - A New Strategy for

Synthesizing Solid Electrolytes for Rechargeable Lithium Batteries. *J. Power Sources* **1995**, *54*, 310−315.
(11) Lin, D.; Liu, W.; Liu, Y.; Lee, H. R.; Hsu, P. C.; Liu, K.; Cui, Y. High Ionic Conductivity of Composite Solid Polymer Electrolyte via In Situ Synthesis of Monodispersed SiO_2 Nanospheres in Poly(ethylene oxide). *Nano Lett.* **2016**, *16*, 459−465.
(12) Wang, G. X.; Yang, L.; Wang, J. Z.; Liu, H. K.; Dou, S. X. Enhancement of ionic conductivity of PEO based polymer electrolyte by the addition of nanosize ceramic powders. *J. Nanosci. Nanotechnol.* **2005**, *5*, 1135−1140.
(13) Abouali, S.; Yim, C. H.; Merati, A.; Abu-Lebdeh, Y.; Thangadurai, V. Garnet-Based Solid-State Li Batteries: From Materials Design to Battery Architecture. *ACS Energy Lett.* **2021**, *6*, 1920−1941.
(14) Itoh, M.; Inaguma, Y.; Jung, W.; Chen, L.; Nakamura, T. High lithium ion conductivity in the perovskite-type compounds. *Solid State Ionics* **1994**, *70*−*71*, 203−207.
(15) Kamaya, N.; Homma, K.; Yamakawa, Y.; Hirayama, M.; Kanno, R.; Yonemura, M.; Kamiyama, T.; Kato, Y.; Hama, S.; Kawamoto, K.; Mitsui, A. A lithium superionic conductor. *Nat. Mater.* **2011**, *10*, 682−686.
(16) Aono, H.; Sugimoto, E.; Sadaoka, Y.; Imanaka, N.; Adachi, G. Ionic-Conductivity of Solid Electrolytes Based on Lithium Titanium Phosphate. *J. Electrochem. Soc.* **1990**, *137*, 1023−1027.
(17) Wu, N.; Chien, P. H.; Qian, Y.; Li, Y.; Xu, H.; Grundish, N. S.; Xu, B.; Jin, H.; Hu, Y. Y.; Yu, G.; Goodenough, J. B. Enhanced Surface Interactions Enable Fast Li(+) Conduction in Oxide/Polymer Composite Electrolyte. *Angew. Chem., Int. Ed.* **2020**, *59*, 4131−4137.
(18) Wu, N.; Chien, P. H.; Li, Y.; Dolocan, A.; Xu, H.; Xu, B.; Grundish, N. S.; Jin, H.; Hu, Y. Y.; Goodenough, J. B. Fast Li(+) Conduction Mechanism and Interfacial Chemistry of a NASICON/Polymer Composite Electrolyte. *J. Am. Chem. Soc.* **2020**, *142*, 2497−2505.
(19) Liu, W.; Liu, N.; Sun, J.; Hsu, P. C.; Li, Y.; Lee, H. W.; Cui, Y. Ionic conductivity enhancement of polymer electrolytes with ceramic nanowire fillers. *Nano Lett.* **2015**, *15*, 2740−2745.
(20) Liu, W.; Lee, S. W.; Lin, D. C.; Shi, F. F.; Wang, S.; Sendek, A. D.; Cui, Y. Enhancing ionic conductivity in composite polymer electrolytes with well-aligned ceramic nanowires. *Nat. Energy* **2017**, *2*, 17035.
(21) Wan, J.; Xie, J.; Kong, X.; Liu, Z.; Liu, K.; Shi, F.; Pei, A.; Chen, H.; Chen, W.; Chen, J.; Zhang, X.; Zong, L.; Wang, J.; Chen, L. Q.; Qin, J.; Cui, Y. Ultrathin, flexible, solid polymer composite electrolyte enabled with aligned nanoporous host for lithium batteries. *Nat. Nanotechnol.* **2019**, *14*, 705−711.
(22) MacGlashan, G. S.; Andreev, Y. G.; Bruce, P. G. Structure of the polymer electrolyte poly(ethylene oxide)$_6$: $LiAsF_6$. *Nat.* **1999**, *398*, 792−794.
(23) Mao, G. M.; Perea, R. F.; Howells, W. S.; Price, D. L.; Saboungi, M. L. Relaxation in polymer electrolytes on the nanosecond timescale. *Nat.* **2000**, *405*, 163−165.
(24) Zou, Z.; Li, Y.; Lu, Z.; Wang, D.; Cui, Y.; Guo, B.; Li, Y.; Liang, X.; Feng, J.; Li, H.; Nan, C. W.; Armand, M.; Chen, L.; Xu, K.; Shi, S. Mobile Ions in Composite Solids. *Chem. Rev.* **2020**, *120*, 4169−4221.
(25) Zheng, J.; Tang, M.; Hu, Y. Y. Lithium Ion Pathway within $Li_7La_3Zr_2O_{12}$-Polyethylene Oxide Composite Electrolytes. *Angew. Chem., Int. Ed.* **2016**, *55*, 12538−12542.
(26) Yang, T.; Zheng, J.; Cheng, Q.; Hu, Y. Y.; Chan, C. K. Composite Polymer Electrolytes with $Li_7La_3Zr_2O_{12}$ Garnet-Type Nanowires as Ceramic Fillers: Mechanism of Conductivity Enhancement and Role of Doping and Morphology. *ACS Appl. Mater. Interfaces* **2017**, *9*, 21773−21780.
(27) Choi, J. H.; Lee, C. H.; Yu, J. H.; Doh, C. H.; Lee, S. M. Enhancement of ionic conductivity of composite membranes for all-solid-state lithium rechargeable batteries incorporating tetragonal $Li_7La_3Zr_2O_{12}$ into a polyethylene oxide matrix. *J. Power Sources* **2015**, *274*, 458−463.
(28) Zheng, J.; Hu, Y.-Y. New insights into the compositional dependence of Li-Ion transport in polymer−ceramic composite electrolytes. *ACS Appl. Mater. Interfaces* **2018**, *10*, 4113−4120.
(29) Wang, L.; Xie, R.; Chen, B.; Yu, X.; Ma, J.; Li, C.; Hu, Z.; Sun, X.; Xu, C.; Dong, S.; Chan, T. S.; Luo, J.; Cui, G.; Chen, L. In-situ visualization of the space-charge-layer effect on interfacial lithium-ion transport in all-solid-state batteries. *Nat. Commun.* **2020**, *11*, 5889.
(30) Cheng, Z.; Liu, M.; Ganapathy, S.; Li, C.; Li, Z. L.; Zhang, X. Y.; He, P.; Zhou, H. S.; Wagemaker, M. Revealing the Impact of Space-Charge Layers on the Li-Ion Transport in All-Solid-State Batteries. *Joule* **2020**, *4*, 1311−1323.
(31) Zheng, J.; Hu, Y. Y. New Insights into the Compositional Dependence of Li-Ion Transport in Polymer-Ceramic Composite Electrolytes. *ACS Appl. Mater. Interfaces* **2018**, *10*, 4113−4120.

https://doi.org/10.1021/acs.jpclett.1c04085
J. Phys. Chem. Lett. 2022, 13, 1500−1505